Preparation and Properties of (BATB–ODPA) Polyimide–Clay Nanocomposite Materials

Jui-Ming Yeh,[1] Chi-Lun Chen,[1] Tai-Hung Kuo,[1] Wen-Fen Su,[1] Hsi-Ya Huang,[1] Der-Jang Liaw,[2] Hsin-Yi Lu,[2] Chi-Fong Liu,[2] Yuan-Hsiang Yu[3]

[1]*Department of Chemistry and Center for Nanotechnology at CYCU, Chung-Yuan Christian University, Chung Li, Taiwan 320, China*
[2]*Department of Chemical Engineering, National Taiwan University of Science and Technology, Taiwan, China*
[3]*Department of Electronic Engineering, Lan-Yan Institute of Technology, I-Lan 261, Taiwan, China*

Received 24 March 2003; accepted 20 June 2003

ABSTRACT: A series of polymer–clay nanocomposite (PCN) materials consisting of 1,4-bis(4-aminophenoxy)-2-*tert*-butylbenzene–4,4′-oxydiphthalic anhydride (BATB–ODPA) polyimide (PI) and layered montmorillonite (MMT) clay were successfully prepared by an *in situ* polymerization reaction through thermal imidization up to 300°C. The synthesized PCN materials were subsequently characterized by Fourier-Transform infrared (FTIR) spectroscopy, wide-angle powder X-ray diffraction (XRD) and transmission electron microscopy (TEM). The effects of material composition on thermal stability, mechanical strength, molecular permeability and optical clarity of bulk PI and PCN materials in the form of membranes were studied by differential scanning calorimetry (DSC), thermogravimetric analysis (TGA), dynamic mechanical analysis (DMA), molecular permeability analysis (GPA) and ultraviolet-visible (UV/VIS) transmission spectra, respectively. © 2004 Wiley Periodicals, Inc. J Appl Polym Sci 92: 1072–1079, 2004

Key words: polyimides; clay; nanocomposites; permeability

INTRODUCTION

Aromatic polyimides (PIs) have traditionally been considered to be thermally stable polymers that display excellent mechanical strength and thermal stability among engineering polymers. During the past decade, research interest in these polymers has increased in response to increasing technological applicability in many fields (e.g. aerospace, automobile, and microelectronics). Recently, significant efforts in the research field of synthesizing high-temperature aromatic PIs has focused on improving their processability and solubility through the synthesis of new diamine or dianhydride monomers. Several modifications to the polyimide backbone (e.g. the introduction of flexible bridging linkages into the polymer backbone,[1,2] the incorporation of bulky substituents along the polymer backbone[3,4]) have led to significant success in preparing soluble PIs.

On the other hand, polymer–clay hybrid nanocomposite materials have evoked great research attention because the dispersing of nanolayered clay, in the form of intercalation or exfoliation, into various polymer matrices has been found to boost thermal stability,[5] mechanical strength,[6] gas barrier,[7] flame resistance[8] and corrosion protection[9–11] properties of bulk polymers. The study of polymer–clay nanocomposites (PCN) can be traced back to the work reported by Toyota's research group in 1990.[12] Currently, there is a considerable number of publications describing the preparation and properties of polyimide–clay nanocomposite[13–17] and soluble polyimide–clay nanocomposite materials.[18–20] Typically, the chemical structure of montmorillonite (MMT) used for PCN preparation consists of two fused silica tetrahedral sheets sandwiching an edge-shared octahedral sheet of either magnesium or aluminum hydroxide. The Na^+ and Ca^{+2} present in the interlayer regions can be replaced by organic cations such as alkylammonium ions through a cationic-exchange reaction to render the hydrophilic silicate layer organophilic, leading to the development of PCN materials.

In this article, a series of PCN materials consisting of 1,4-bis(4-aminophenoxy)-2-*tert*-butylbenzene–4,4′-oxydiphthalic anhydride (BATB–ODPA) polyimide and layered MMT clay were successfully prepared by an *in situ* polymerization through thermal imidization up to 300°C. The synthesized PCN materials were subsequently characterized by Fourier-transform infrared (FTIR) spectroscopy, wide-angle powder X-ray diffraction (XRD) and transmission electron microscopy (TEM).

The effects of material composition on thermal stability, mechanical strength, molecular permeability and optical clarity of bulk PI and PCN materials in the form of membranes were studied by differential scan-

Correspondence to: J.-M. Yeh (juiming@cycu.edu.tw.).

Journal of Applied Polymer Science, Vol. 92, 1072–1079 (2004)

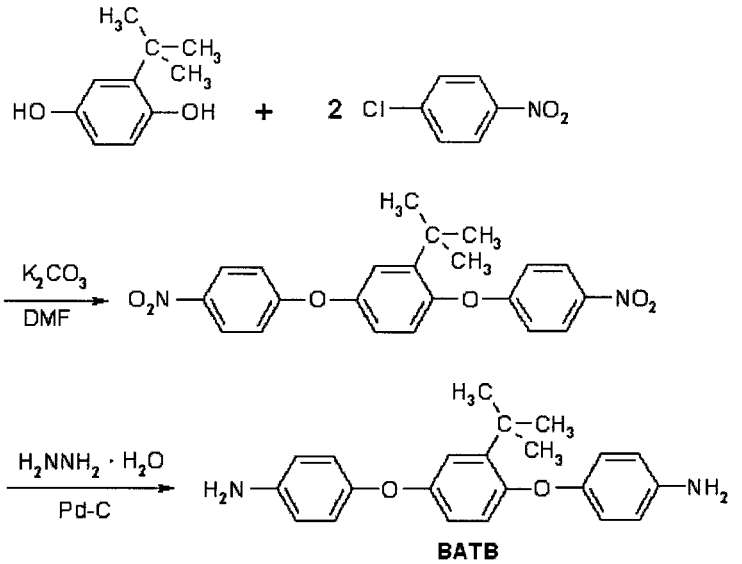

Scheme 1

ning calorimetry (DSC), thermogravimetric analysis (TGA), dynamic mechanical analysis (DMA), molecular permeability analysis (GPA), and ultraviolet-visible transmission spectra, respectively.

EXPERIMENTAL

Chemicals and instrumentation

4,4′-oxydiphthalic anhydride (ODPA), (Riedel-de Haën, 98%), *tert*-butylhydroquinone (Janssen), P-chloronitrobenzene (Merck), anhydrous potassium carbonate (Janssen), hydrazine monohydrate (Janssen), 10% palladium on activated carbon (Merck), *N,N*-dimethylacetamide (DMAc), (Riedel-de Haën, > 99%), 4,4-oxydianiline (ODA) (Fluka, >98%), and hydrochloric acid (Riedel-de Haën, 37%) were used as received without further purification. MMT clay (Kunipia-F), supplied by Industrial Technology Research Institute (ITRI), had a CEC value of 114 mEq/100 g.

FTIR spectra were measured on pressed KBr pellets using a JASCO FT/IR-460 plus spectrometer. Wide-angle XRD study of the samples was performed with a Rigaku D/MAX-3C OD-2988N X-ray diffractometer with a copper target and Ni filter at a scanning rate of 4°/min. The samples for TEM study were first prepared by putting membranes of PCN materials into epoxy resin capsules followed by curing the epoxy resin at 100°C for 24 h in a vacuum oven. Then the cured epoxy resins containing PCN materials were microtomed with a Reichert–Jumg Ultracut-E into 60–90 nm thick slices. Subsequently, one layer of carbon of about 10 nm in thickness was deposited onto these slices on mesh 100 copper nets for TEM observations on a JEOL-200FX with an acceleration voltage of 120 kV.

A Perkin–Elmer thermal analysis system equipped with model 7 DSC and model 7/DX. TGA was employed for thermal analyses under an N_2 flow. The programmed heating rate was 20°C/min. DMA of PCN membranes was carried out from 0 to 350°C with a Perkin–Elmer 7 Serial analyzer at a heating rate of 10°C/min and a frequency of 1 Hz. A Yanagimoto Co., Ltd gas permeability analyzer (model GTR 10) was employed to perform the permeation experiments of oxygen gas and water vapor. UV/VIS transmission spectra were obtained using a Hitachi U-2000 UV/VIS spectrometer.

Synthesis of diamine monomer (BATB)

The diamines were synthesized through the aromatic nucleophilic substitution of corresponding diols with *p*-chloronitrobenzene or *p*-fluoronitrobenzene in the presence of potassium carbonate, followed by catalytic reduction with hydrazine monohydrate/10% Pd/C. The procedure was as follows:[21] a solution of *tert*-butylhydroquinone (41.5 g, 0.25 mol), *p*-chloronitrobenzene (81.9 g, 0.52 mol), potassium carbonate (79.4 g, 0.57 mol) and *N,N*-dimethylformamide (DMF, 300 mL) was refluxed for 8 h. The mixture was precipitated in an ethanol–water mixture, and the crude dinitro intermediate was recrystallized from glacial acetic acid. A solution of the obtained dinitro compound (57.1 g, 0.14 mol), 0.3 g of 10% Pd on active carbon (10% Pd/C), and 400 mL of ethanol was added dropwise to hydrazine monohydrate (130 mL) at 85°C and then refluxed for 24 h. The mixture was filtered to remove 10% Pd/C. After cooling, the precipitated crystals (BATB) were isolated by filtration and recrystallized from ethanol. The flowchart of the reaction is listed as Scheme 1.

Preparation of (BATB–ODPA) PI membrane through thermal imidization

A typical procedure of preparing PI by thermal imidization was as follows: ODPA (0.155 g, 0.5 mmole) in DMAc (3 mL) was gradually added to a stirred solution of BATB (0.174 g, 0.5 mmole) in DMAc (3 mL). The mixture was stirred at room temperature for 6 h to form poly(amic acid). A membrane was cast from the poly(amic acid) solution onto a glass plate and subsequently heated for 2 h at 80°C, 2 h at 200°C and 2 h at 300°C to convert the poly(amic acid) into a PI membrane.

Preparation of organophilic clay

The organophilic clay was prepared by a cationic-exchange reaction between the sodium cations of MMT clay and a diamine of the intercalating agent, 4,4-oxydianiline. The equation used to calculate the amount of intercalating agent for the cationic-exchange reaction is as follows:

$$\frac{114}{100} \times 5\text{g (MMT)} \times 1.5 = \frac{X}{\text{Mw of intercalating agent}} \times 1 \times 1000$$

where X is the amount of intercalating agent used, 114/100 represented the CEC value per 100 g of MMT, and 1.5 (>1) indicates that an excess amount of intercalating agent was used. Typically, 5 g of MMT clay with a CEC value of 114 mEq/100 g was stirred in 500 mL of distilled water (beaker A) at room temperature overnight. A separate solution containing 2.0 g of intercalating agent in another 100 mL of distilled water (beaker B) was kept under magnetic stirring, followed by the addition of 1.0*M* HCl aqueous solution to adjust the pH value to about 3≈4. After stirring for 1 h, the protonated amino acid solution (beaker B) was added at a rate of approximately 10 mL/min with vigorous stirring to the MMT suspension (beaker A). The mixture was stirred overnight at room temperature. The organophilic clay was recovered by ultracentrifuging (9000 rpm, 30 min) and filtering the solution in a Buchner funnel. Purification of products was performed by washing and filtering samples at least five times to remove any excess ammonium ions.

In situ polymerization of PCNs by thermal imidization

A procedure for the preparation of PCNs by thermal imidization is shown in Scheme 2: an appropriate amount of organophilic clay with respect to PI (1 wt %, 3 wt %, 5 wt %, 7 wt %, and 10 wt %) was introduced into 6 mL of DMAc under magnetic stirring for 24 h at room temperature. Diamine monomer BATB (0.348 g, 1 mmole) was subsequently added to the solution, which was stirred for another 24 h. Then a separate solution containing ODPA (0.310 g, 1 mmole) in DMAc (6 mL) under magnetic stirring was gradually added to the stirred BATB solution. The mixture was further stirred at room temperature for 24 h to give a PCN solution. The prepared poly(amic acid)–clay nanocomposite solution was subsequently filtered with a 0.45 μm hydrophilic PVDF filter (Millpore Millev-HV) and cast onto 4 pcs of glass plate (5 cm × 5 cm, ≈3c.c./pcs). Thermal imidization was performed for 2 h at 80°C, 1 h at 200°C and 1 h at 300°C to convert the poly(amic acid)–clay nanocomposite solution into a PCN membrane.

Preparation of membranes and barrier property measurements

The method used to prepare PCN membranes for measurement of barrier property was the same as that described above. The prepared sample-coated glass substrate was immersed in boiling water for 2 h to give PCN membranes.

Oxygen permeability of the membrane was determined using the Yanco GTR-10 gas permeability analyzer. Gas permeability was calculated using the following equation:

$$P = l/(p_1 - p_2) \times \frac{q/t}{A}$$

where P is the gas permeability [cm^3(STP)-cm/cm^2-s-cmHg], q/t is the volumetric flow rate of gas permeate [cm^3(STP)/s], l is the membrane thickness (cm), A is the effective membrane area (cm^2), and p_1 and p_2 are the pressures (cmHg) on the high pressure and low pressure sides of the membrane, respectively. The rate of transmission of O_2 was obtained by gas chromatography, from which the air permeability was calculated. Measurement of H_2O permeability was performed on the same apparatus, except that the feed solution was not in contact with the membrane. The feed solution was vaporized first and subsequently permeated through the membrane with an effective area of ≈10.2 cm^2. The permeation rate was determined by measuring the weight of permeate.

RESULTS AND DISCUSSION

MMT was shown to have a high swelling capacity, which is important for efficient intercalation of the polymer, and it is composed of stacked silicate sheets that boost many properties of bulk polymers. The composition of the PCN materials was varied from 0 to 10 wt % of clay with respect to polyimide content, as summarized in Table I.

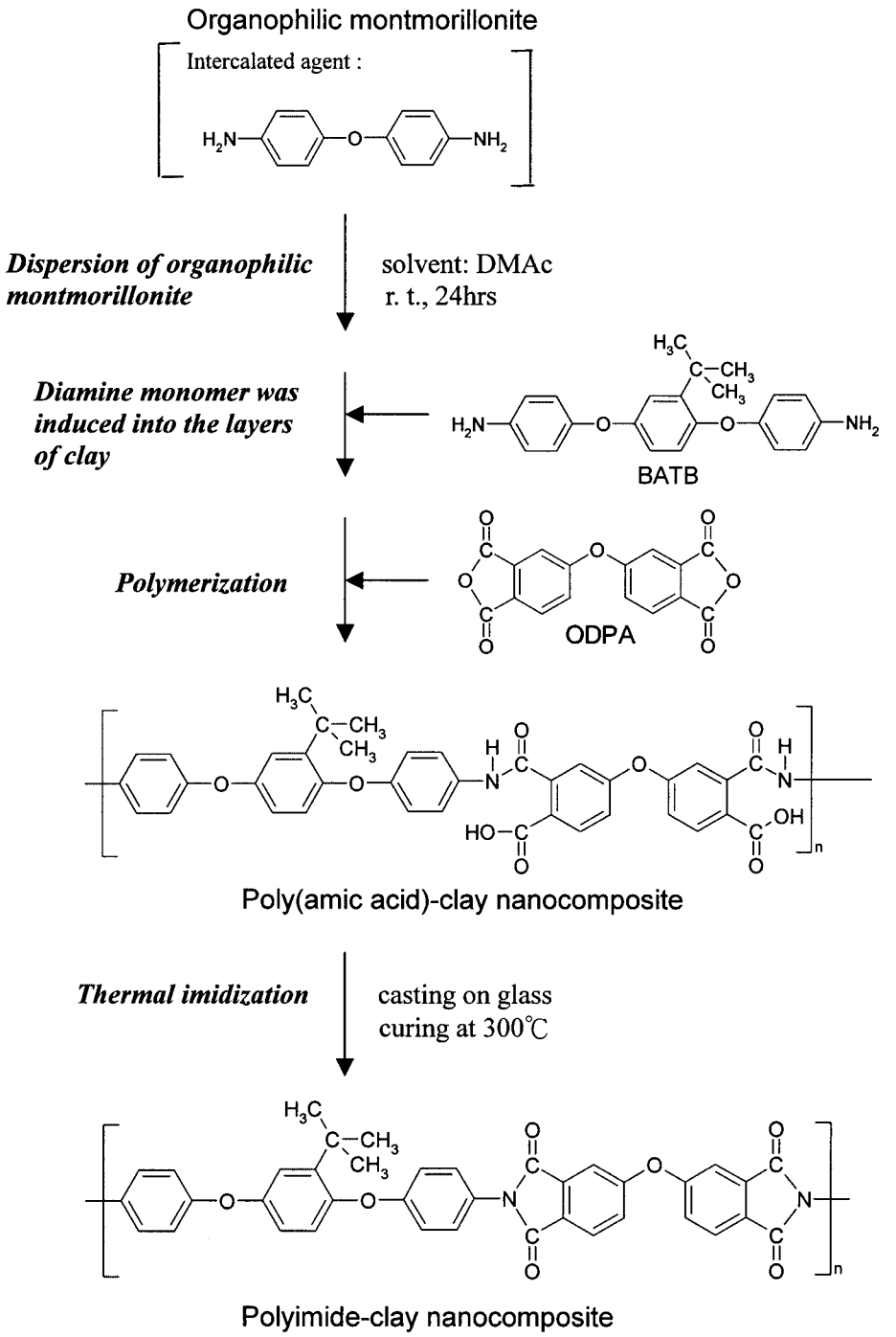

Scheme 2

Characterization

Typical FTIR spectra for the reactions of BATB and ODPA at 80°C, 100°C, 200°C and 300°C are shown in Figure 1. The spectrum shown in Figure 1(a) at 80°C is from the poly(amic acid) film (before imidization), in which the bands at 1657 and 1542 cm^{-1} correspond to the stretching of the carbonyl groups.[22] The absorption at 3200≈3400 cm^{-1} could be from the -COOH and -NH groups, as shown in Figure 1(b) at 80°C. The spectrum shown in Figure 1(a) at 300°C is from the polyimide membrane (after imidization). The obvious appearance of the band at 1777 cm^{-1}, which is characteristic of C═O stretching in imide groups, and the band at 1374 cm^{-1}, which is characteristic of C—N stretching in imide groups, the disappearance of the 1657 and 1542 cm^{-1} bands, and the decrease of the 3200≈3400 cm^{-1} clearly indicate that the poly(amic acid) was converted to polyimide after thermal treat-

TABLE I
Relations of Composition of Polyimide (BATB–ODPA)–MMT Clay Nanocomposite Materials to Thermal, Mechanical and Barrier Properties Measured by DSC, TGA and DMA, and GPA

Compound Code	Feed Composition (Wt %)		Thermal Properties[a] (°C)			Mechanical Strength[b] (Pa)	Barrier Properties[c] (Barrier)		(g/m² · h)
	Polyimide	MMT	T_g	T_d 5%	Char Yield (%)	E′	O_2	N_2	H_2O
PI	100	0	377.96	457.7	44.77	2.7×10^7	3.869	0.721	211
PCN1	99	1	388.27	458.1	47.58	3.9×10^7	1.598	0.31	147
PCN3	97	3	388.54	—[d]	—[d]	—	—	—	116
PCN5	95	5	381.35	484.5	50.62	4.2×10^7	0.866	0.167	83
PCN7	93	7	—	545.2	60.05	—	—	—	—
PCN10	90	10	379.35	—[d]	—[d]	4.0×10^7	0.509	0.09	—

[a] T_g was determined by DSC, T_d and char yield was determined by TGA.
[b] Storage modulus (E′) was determined by DMA.
[c] Barrier property of membranes was determined by gas permeability analyzer (GPA).
[d] Data unavailable.

ment. Figure 2 shows the representative FTIR spectra for polyimide, PCN1, PCN5, PCN10 and organophilic clay. The characteristic vibration bands of MMT clay are shown at 1040 cm^{-1} (Si—O), 523 cm^{-1} (Al—O) and 464 cm^{-1} (Mg—O).[9–11] As the loading of MMT clay was increased, the intensity of MMT clay bands became much stronger in the FTIR spectra of PCN materials.

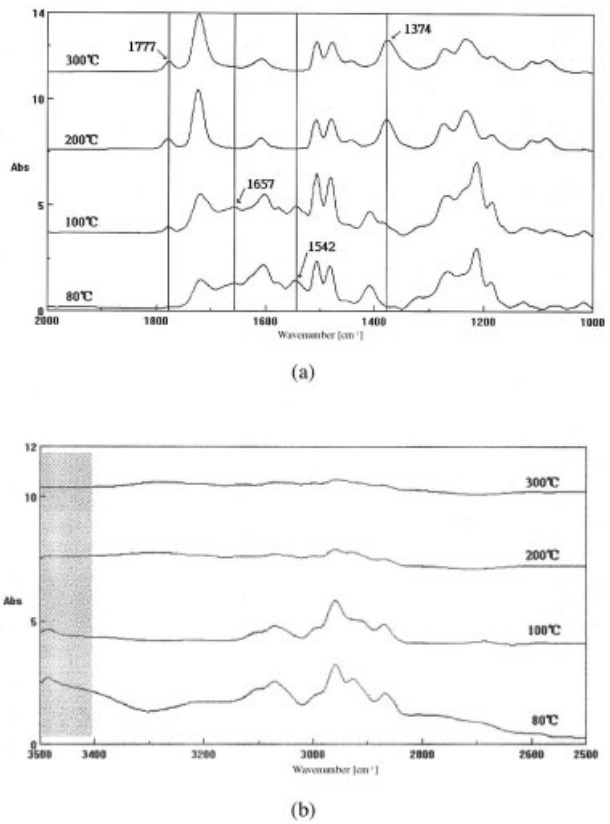

Figure 1 FTIR spectra for the reactions of BATB and ODPA by thermal imidization at 80°C, 100°C, 200°C, and 300°C.

Figure 3(a) illustrates the wide-angle powder XRD patterns of organophilic clay, PI and a series of PCN materials. Raw Na^+-MMT was found to show a diffraction peak at $2\theta = 7.10°$ (d spacing = 1.24 nm). For PCN1, there was a lack of any diffraction peak at $2\theta = 2–10°$ as opposed to the diffraction peak at $2\theta = 6.02°$ (d spacing = 1.45 nm) for organophilic clay, implying the possibility of exfoliated organophilic clay platelets embedded in the PI matrix. When the amount of organoclay increased to 5%, there was a small peak appearing at $2\theta = 6.00°$, corresponding to a d spacing of 1.48 nm. This indicates that there may be a small amount of organoclay that cannot be exfoliated in PI and exists in the form of an intercalated layer structure. In Figure 4, the TEM of PCN materials incorporated with 5 wt % clay reveal that the nanocomposites displayed a combination of nano-morphology. Individual silicate layers, along with two and three layer stacks, were found to be exfoliating in the PI matrix. Besides, some tactoids of larger intercalated multilayers can also be identified in the figure.

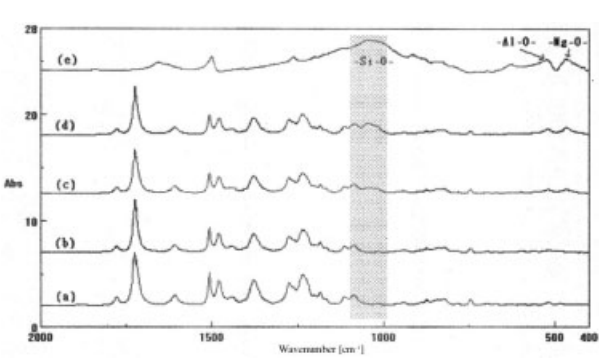

Figure 2 FTIR spectra for (a) polyimide (b) PCN1 (c) PCN5 (d) PCN10 (e) organophilic clay.

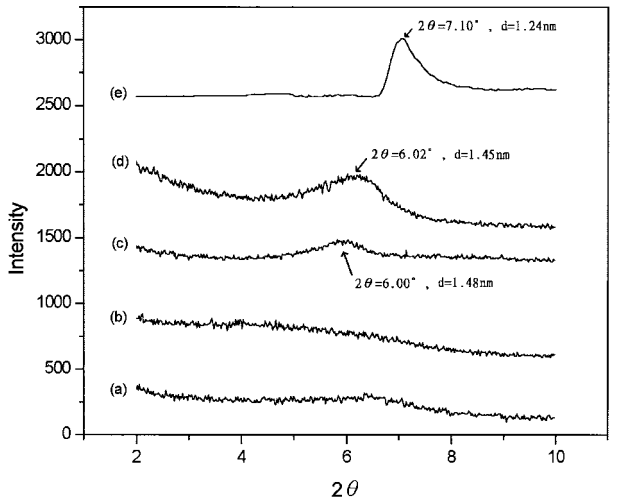

Figure 3 Wide-angle powder X-ray diffraction patterns for (a) polyimide (b) PCN1 (c) PCN5 (d) organophilic clay (e) Na^{+}-MMT.

Thermal properties of fine powders

Figure 5 shows typical TGA thermograms of weight loss as a function of temperature for PI and the PCN materials, as measured under a N_2 atmosphere. The TGA curves of PI and PCN membranes prepared from thermal imidization show one major weight loss at 400≈600°C, which was attributed to the structural decomposition of the polymer. The thermal decomposition temperature of those PCN membranes was found to shift more toward the higher temperature range than that of bulk PI, which confirmed the enhancement of thermal stability of the intercalated polymer.[10] It should be noted that the char yield of PCN materials (>40%) was found to be slightly higher

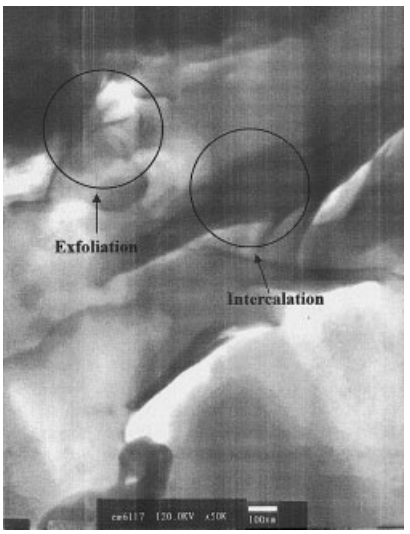

Figure 4 Transmission electron micrograph image of PCN5.

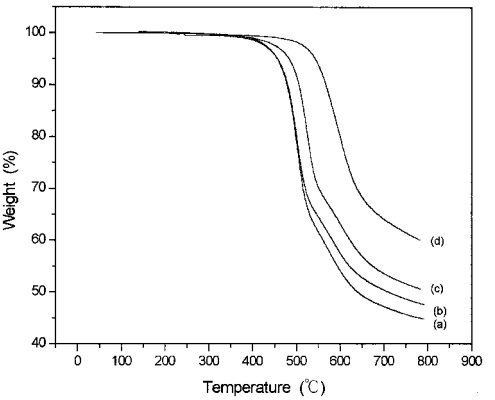

Figure 5 TGA curves for (a) PI (b) PCN1 (c) PCN5 (d) PCN7.

than that of PI, implying that PCN materials may showed enhanced flame resistant properties relative to bulk PI. DSC traces of bulk PI and PCN materials are shown in Figure 6. PI exhibited an endotherm at 377.96°C, corresponding to the T_g of PI. PCN1 showed an increased T_g compared to pure PI. This was tentatively attributed to the confinement of the intercalated polymer chains within the clay galleries, which prevented segmental motions of the polymer chains.[10] Moreover, the T_g values of PCN materials were found to increase up to 3 wt % (≈388.54°C). However, a further increase of clay loading (e.g. 5 wt %, 10 wt %) was found to decrease the T_g, which is consistent with results reported by other groups.[15]

Mechanical properties of membranes

DMA of the PI–clay nanocomposite materials was carried out to investigate the effect of the clay nanolayers on the thermomechanical properties of the polyimide membrane. The storage moduli (E') with various clay contents are shown in Figure 7. It was confirmed that the storage modulus increased with the increase of the clay content up to 5 wt % loading. The moduli were 2.7×10^7, 3.9×10^7, 4.2×10^7, and

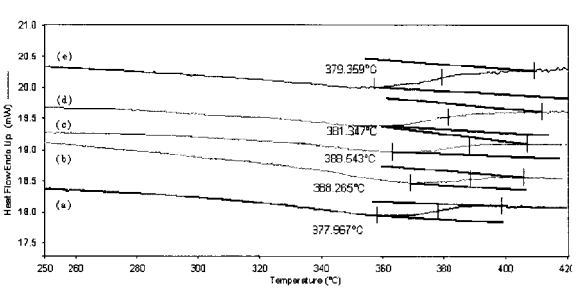

Figure 6 DSC curves for (a) polyimide (b) PCN1 (c) PCN3 (d) PCN5 (e) PCN10.

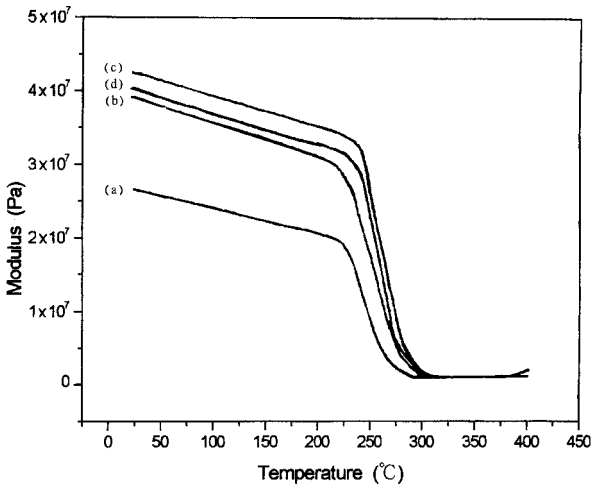

Figure 7 Relationship between the storage modulus (E') and temperature as obtained from DMA measurements on the free-standing film of (a) PI (b) PCN1 (c) PCN5 (d) PCN10.

4.0×10^7 Pa at the clay content of 0, 1, 5, and 10 wt %, respectively.

Molecular permeability of membranes

The membranes of PI and PCN materials used for the molecular permeability measurements were prepared with membrane thickness of ≈50 μm. The H_2O molecular permeability property of PCN membranes showed that the dispersing of the clay platelets promoted the molecular barrier of H_2O gas. Furthermore, it should be noted that a further increase of clay loading resulted in further enhancement of the molecular barrier property of PCN materials. A large value of permeability was found at higher temperatures, as illustrated in Figure 8. Furthermore, we also found

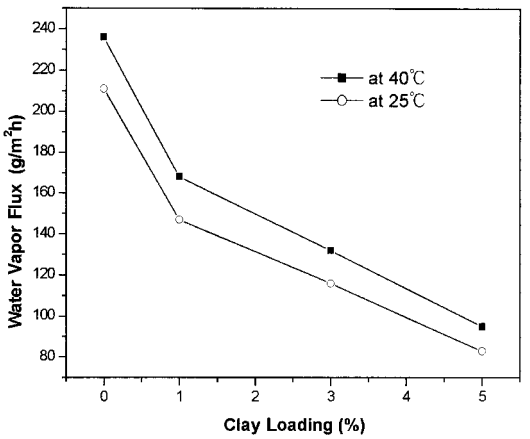

Figure 8 Permeability of water vapor as a function of the MMT clay content in the polyimide-clay nanocomposite materials at various temperature.

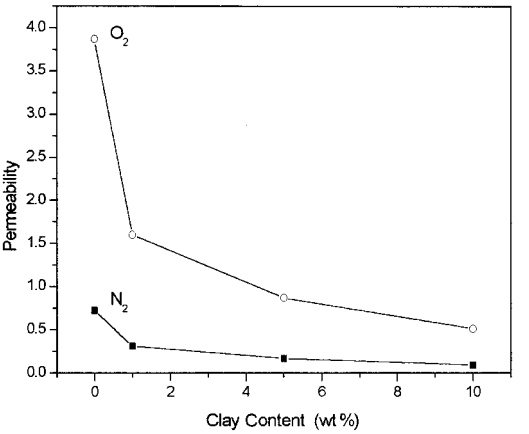

Figure 9 Permeability of O_2, N_2 as a function of the MMT clay content in the polyimide-clay nanocomposite materials at 30°C.

that the incorporation of clay platelets into the PI matrix resulted in a decrease of O_2 and N_2 permeability in PCN membranes, as shown in Figure 9. For example, PCN membranes at low clay loading (1 wt %) showed approximately 56% reduction in O_2 permeability compared to bulk PI membrane.

Optical clarity of membranes

In this study, optical clarity of membranes was found to remain high at low clay contents (e.g. PCN1) because of the nanoscale dispersion of clay platelets into the PI matrix, which may yield primarily exfoliated composites.[10] Figure 10 shows the UV/VIS transmission spectra of pure PI and PCNs with 1 and 5 wt % MMT. These membranes have thicknesses of ≈40 μm. The spectra of PCN1 showed that the visible region (400–700 nm) was almost completely unaffected by the presence of the clay and retained high transparency of PI. However, the spectra of PCN5 exhibiting low transparency of the PI are evidence of the primarily intercalated composites.[10] For the ultraviolet wave-

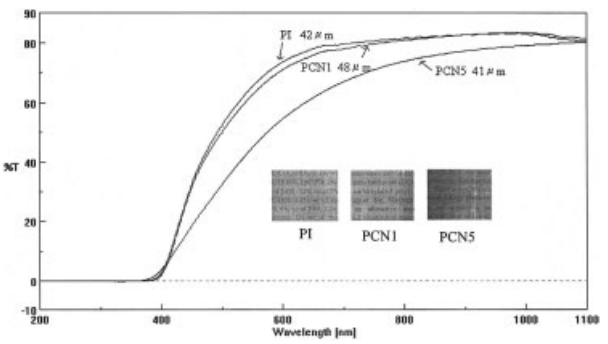

Figure 10 UV/VIS transmission spectra of PI and PI-clay nanocomposite containing 1 and 1 and 5 wt % MMT.

length, there was strong scattering and/or absorption, leading to a lower transmission of the UV light.

CONCLUSIONS

A series of PCN materials consisting of polyimide (PATB–ODPA) and inorganic MMT clay platelets was prepared by effectively dispersing the inorganic nanolayers of MMT clay in an organic PI matrix by an *in situ* polymerization. The synthesized PCN materials were characterized by FTIR, wide-angle powder XRD and TEM.

The effects of material composition on thermal stability, mechanical strength, molecular barrier and optical clarity of PI and PCN materials, in the form of membranes, were studied by DSC and TGA, DMA, GPA, and UV/VIS transmission spectra, respectively. Dispersal of MMT clay platelets into the PI matrix was found to boost the thermal stability, as by the enhancement of thermal decomposition temperature (T_d) and glass transition temperature (T_g) of PI based on the TGA and DSC studies. It was confirmed that the storage modulus of the membranes increased with increasing clay content based on DMA studies. The incorporation of clay platelets into PI membrane resulted in an enhancement of O_2 and H_2O molecular barrier property based on gas permeability analysis. Higher clay loading in PI membrane led to a significant decrease of optical clarity based on the UV/VIS transmission spectra studies.

The financial support of this research by the NSC 90-2113-M-033-010 is gratefully acknowledged.

REFERENCES

1. Feld, W. A.; Ramalingam, B.; Harris, F. W. J Polym Sci Part A: Polym Chem 1983, 21, 319.
2. Imai, Y.; Maldar, N. N.; Kakimoto, M. J Polym Sci Part A: Polym Chem 1984, 22, 2189.
3. Jadhav, J. Y.; Preston, J.; Krigbaum, W. R. J Polym Sci Part A: Polym Chem 1989, 27, 1175.
4. Nagara, N.; Tsutsumi, N.; Kyotsukuri, T. J Polym Sci Part A: Polym Chem 1988, 26, 235.
5. Lan, T.; Kaviratna, P. D.; Pinnavaia, T. J Chem Mater 1994, 6, 573.
6. Tyan, H.-L.; Liu, Y.-C.; Wei, K.-H. Chem Mater 1999, 11, 1942.
7. Wang, Z.; Pinnavaia, T. J Chem Mater 1998, 10, 3769.
8. Gilman, J. W.; Jackson, C. L.; Morgan, A. B.; Hayyis, R., Jr.; Manias, E.; Giannelis, E. P.; Wuthenow, M.; Hilton, D.; Phillips, S. H. Chem Mater 2000, 12, 1866.
9. Yeh, J.-M.; Liou, S.-J.; Lai, C. Y.-Y.; Wu, P.-C.; Tsai, T.-Y. Chem Mater 2001, 13, 1131.
10. Yeh, J.-M.; Liou, S.-J.; Lin, C.-Y.; Cheng, C.-Y.; Chang, Y. W. Chem Mater 2002, 14, 154.
11. (a) Yeh, J.-M.; Chen, C.-L.; Chen, Y. –C.; Ma, C.-Y.; Lee, K.-R.; Wei, Y.; Li, S. Polymer 2002, 43, 2729. (b) Yeh, J.-M.; Chin, C.-P. J Appl Polym Sci 2003, 88, 1072.
12. Usuki, A.; Kawasumi, M.; Kojima, Y.; Okada, A.; Karauchi, T.; Kamigaito, O. J Mater Res 1993, 8, 1774.
13. Gu, A.; Kuo, S.-W.; Chang, F.-C. J Appl Polym Sci 2001, 79, 1902.
14. Agag, T.; Koga, T.; Takeichi, T. Polymer 2001, 42, 3399.
15. Tyan, H.-L.; Wei, K.-H.; Hsieh, T. E. J Polym Sci Part B: Polym Physics 2000, 38, 2873.
16. Morgan, A. B.; Gilman, J. W.; Jackson, C. L. Macromolecules 2001, 34, 2735.
17. Tyan, H.-L.; Leu, C.-M.; Wei, K.-H. Chem Mater 2001, 13, 222.
18. Huang, J.-C.; Zhu, Z.-K.; Ma, X.-D.; Qian, X.-F.; Yin, J. J Mater Sci 2001, 36, 871.
19. Hsiao, S.-H.; Liou, G.-S.; Chang, L.-M. J Appl Polym Sci 2001, 80, 2067.
20. Yang, Y.; Zhu, Z.-K.; Yin, J.; Wang, X.-Y.; Qi, Z.-E. Polymer 1999, 40, 4407.
21. Liaw, D. J.; Liaw, B. Y. Polym J 1996, 28, 970.
22. Tyan, H.-L.; Liu, Y.-C.; Wei, K.-H. Polymer 1999, 40, 4877.